

# Cavitation Resistance in Seedless Vascular Plants: The Structure and Function of Interconduit Pit Membranes<sup>1</sup>[W][OPEN]

Craig Brodersen, Steven Jansen, Brendan Choat, Christopher Rico, and Jarmila Pittermann\*

School of Forestry and Environmental Studies, Yale University, New Haven, Connecticut 06511 (C.B.); Institute for Systematic Botany and Ecology, Ulm University, 89081 Ulm, Germany (S.J.); University of Western Sydney, Hawkesbury Institute for the Environment, Richmond, New South Wales 2753, Australia (B.C.); and Department of Ecology and Evolutionary Biology, University of California, Santa Cruz, California 95064 (C.R., J.P.)

Plant water transport occurs through interconnected xylem conduits that are separated by partially digested regions in the cell wall known as pit membranes. These structures have a dual function. Their porous construction facilitates water movement between conduits while limiting the spread of air that may enter the conduits and render them dysfunctional during a drought. Pit membranes have been well studied in woody plants, but very little is known about their function in more ancient lineages such as seedless vascular plants. Here, we examine the relationships between conduit air seeding, pit hydraulic resistance, and pit anatomy in 10 species of ferns (pteridophytes) and two lycophytes. Air seeding pressures ranged from  $0.8 \pm 0.15$  MPa (mean  $\pm$  SD) in the hydric fern *Athyrium filix-femina* to  $4.9 \pm 0.94$  MPa in *Psilotum nudum*, an epiphytic species. Notably, a positive correlation was found between conduit pit area and vulnerability to air seeding, suggesting that the rare-pit hypothesis explains air seeding in early-diverging lineages much as it does in many angiosperms. Pit area resistance was variable but averaged  $54.6 \text{ MPa s m}^{-1}$  across all surveyed pteridophytes. End walls contributed 52% to the overall transport resistance, similar to the 56% in angiosperm vessels and 64% in conifer tracheids. Taken together, our data imply that, irrespective of phylogenetic placement, selection acted on transport efficiency in seedless vascular plants and woody plants in equal measure by compensating for shorter conduits in tracheid-bearing plants with more permeable pit membranes.

Water transport in plants occurs under tension, which renders the xylem susceptible to air entry. This air seeding may lead to the rupture of water columns (cavitation) such that the air expands within conduits to create air-vapor embolisms that block further transport. (Zimmermann and Tyree, 2002). Excessive embolism such as that which occurs during a drought may jeopardize leaf hydration and lead to stomatal closure, overheating, wilting, and possibly death of the plant (Hubbard et al., 2001; Choat et al., 2012; Schymanski et al., 2013). Consequently, strong selection pressure resulted in compartmentalized and redundant plant vascular networks that are adapted to a species habitat water availability by way of life history strategy (i.e. phenology) or resistance to air seeding (Tyree et al., 1994; Mencuccini et al., 2010; Brodersen et al., 2012). The spread of drought-induced embolism is limited primarily by pit membranes, which are permeable, mesh-like regions in the primary cell wall that connect two adjacent conduits. The construction of the

pit membrane is such that water easily moves across the membrane between conduits, but because of the small membrane pore size and the presence of a surface coating on the membrane (Pesacreta et al., 2005; Lee et al., 2012), the spread of air and gas bubbles is restricted up to a certain pressure threshold known as the air-seeding pressure (ASP). When xylem sap tension exceeds the air-seeding threshold, air can be aspirated from an air-filled conduit into a functional water-filled conduit through perhaps a large, preexisting pore or one that is created by tension-induced membrane stress (Rockwell et al., 2014). Air seeding leads to cavitation and embolism formation, with emboli potentially propagating throughout the xylem network (Tyree and Sperry, 1988; Brodersen et al., 2013). So, on the one hand, pit membranes are critical to controlling the spread of air throughout the vascular network, while on the other hand, they must facilitate the efficient flow of water between conduits (Choat et al., 2008; Domec et al., 2008; Pittermann et al., 2010; Schulte, 2012). Much is known about such hydraulic tradeoffs in the pit membranes of woody plants, but comparatively little data exist on seedless vascular plants such as ferns and lycophytes. Given that seedless vascular plants may bridge the evolutionary transition from bryophytes to woody plants, the lack of functional data on pit membrane structure in early-derived tracheophytes is a major gap in our understanding of the evolution of plant water transport.

In woody plants, pit membranes fall into one of two categories: the torus-margo type found in most gymnosperms

<sup>1</sup> This work was supported by the National Science Foundation (grant no. IOS-1027410 to J.P.), the Save the Redwoods League (to C.R.), and the Alexander von Humboldt Foundation (to B.C.).

\* Address correspondence to jpitterm@ucsc.edu.

The author responsible for distribution of materials integral to the findings presented in this article in accordance with the policy described in the Instructions for Authors ([www.plantphysiol.org](http://www.plantphysiol.org)) is: Jarmila Pittermann (jpitterm@ucsc.edu).

[W] The online version of this article contains Web-only data.

[OPEN] Articles can be viewed online without a subscription.

[www.plantphysiol.org/cgi/doi/10.1104/pp.113.226522](http://www.plantphysiol.org/cgi/doi/10.1104/pp.113.226522)

and the homogenous pit membrane characteristic of angiosperms (Choat et al., 2008; Choat and Pittermann, 2009). In conifers, water moves from one tracheid to another through the margo region of the membrane, with the torus sealing the pit aperture should one conduit become embolized. Air seeding occurs when water potential in the functional conduit drops low enough to dislodge the torus from its sealing position, letting air pass through the pit aperture into the water-filled tracheid (Domec et al., 2006; Delzon et al., 2010; Pittermann et al., 2010; Schulte, 2012; but see Jansen et al., 2012). Across north-temperate conifer species, larger pit apertures correlate with lower pit resistance to water flow ( $r_{\text{pit}}$ ; MPa s m<sup>-1</sup>), but it is the ratio of torus-aperture overlap that sets a species cavitation resistance (Pittermann et al., 2006, 2010; Domec et al., 2008; Hacke and Jansen, 2009). A similar though mechanistically different tradeoff exists in angiosperm pit membranes. Here, air seeding reflects a probabilistic relationship between membrane porosity and the total area of pit membranes present in the vessel walls. Specifically, the likelihood of air aspirating into a functional conduit is determined by the combination of xylem water potential and the diameter of the largest pore and/or the weakest zone in the cellulose matrix in the vessel's array of pit membranes (Wheeler et al., 2005; Hacke et al., 2006; Christman et al., 2009; Rockwell et al., 2014). As it has come to be known, the rare-pit hypothesis suggests that the infrequent, large-diameter leaky pore giving rise to that rare pit reflects some combination of pit membrane traits such as variation in conduit membrane area (large or small), membrane properties (tight or porous), and hydrogel membrane chemistry (Hargrave et al., 1994; Choat et al., 2003; Wheeler et al., 2005; Hacke et al., 2006; Christman et al., 2009; Lee et al., 2012; Plavcová et al., 2013; Rockwell et al., 2014). The maximum pore size is critical because, per the Young-Laplace law, the larger the radius of curvature, the lower the air-water pressure difference under which the contained meniscus will fail (Jarbeau et al., 1995; Choat et al., 2003; Jansen et al., 2009). Consequently, angiosperms adapted to drier habitats may exhibit thicker, denser, smaller, and less abundant pit membranes than plants occupying regions with higher water availability (Wheeler et al., 2005; Hacke et al., 2007; Jansen et al., 2009; Lens et al., 2011; Scholz et al., 2013). However, despite these qualitative observations, there is no evidence that increased cavitation resistance arrives at the cost of higher  $r_{\text{pit}}$ . Indeed, the bulk of the data suggest that prevailing pit membrane porosity is decoupled from the presence of the single largest pore that allows air seeding to occur (Choat et al., 2003; Wheeler et al., 2005; Hacke et al., 2006, 2007).

As water moves from one conduit to another, pit membranes offer considerable hydraulic resistance throughout the xylem network. On average,  $r_{\text{pit}}$  contributes 64% and 56% to transport resistance in conifers and angiosperms, respectively (Wheeler et al., 2005; Pittermann et al., 2006; Sperry et al., 2006). In conifers, the average  $r_{\text{pit}}$  is estimated at  $6 \pm 1$  MPa s m<sup>-1</sup>, almost 60 times

lower than the  $336 \pm 81$  MPa s m<sup>-1</sup> computed for angiosperms (Wheeler et al., 2005; Hacke et al., 2006; Sperry et al., 2006). Presumably, the high porosity of conifer pits compensates for the higher transport resistance offered by a vascular system composed of narrow, short, single-celled conduits (Pittermann et al., 2005; Sperry et al., 2006).

Transport in seedless vascular plants presents an interesting conundrum because, with the exception of a handful of species, their primary xylem is composed of tracheids, the walls of which are occupied by homogenous pit membranes (Gibson et al., 1985; Carlquist and Schneider, 2001, 2007; but see Morrow and Dute, 1998, for torus-margo membranes in *Botrychium* spp.). At first pass, this combination of traits appears hydraulically maladaptive, but several studies have shown that ferns can exhibit transport capacities that are on par with more recently evolved plants (Wheeler et al., 2005; Watkins et al., 2010; Pittermann et al., 2011, 2013; Brodersen et al., 2012). Certainly, several taxa possess large-diameter, highly overlapping conduits, some even have vessels such as *Pteridium aquilinum* and many species have high conduit density, all of which could contribute to increased hydraulic efficiency (Wheeler et al., 2005; Pittermann et al., 2011, 2013). But how do the pit membranes of seedless vascular plants compare? Scanning electron micrographs of fern and lycopod xylem conduits suggest that they are thin, diaphanous, and susceptible to damage during specimen preparation (Carlquist and Schneider 2001, 2007). Consistent with such observations, two estimates of  $r_{\text{pit}}$  imply that  $r_{\text{pit}}$  in ferns may be significantly lower than in angiosperms; Wheeler et al. (2005) calculated  $r_{\text{pit}}$  in the fern *Pteridium aquilinum* at 31 MPa s m<sup>-1</sup>, while Schulte et al. (1987) estimated  $r_{\text{pit}}$  at 1.99 MPa s m<sup>-1</sup> in the basal fern *Psilotum nudum*. The closest structural analogy to seedless vascular plant tracheids can be found in the secondary xylem of the early-derived vesselless angiosperms, in which tracheids possess homogenous pit membranes with  $r_{\text{pit}}$  values that at 16 MPa s m<sup>-1</sup> are marginally higher than those of conifers (Hacke et al., 2007). Given that xylem in seedless vascular plants is functionally similar to that in vesselless angiosperms, we expected convergent  $r_{\text{pit}}$  values in these two groups despite their phylogenetic distance. We tested this hypothesis, as well as the intrinsic cavitation resistance of conduits in seedless vascular plants, by scrutinizing the pit membranes of ferns and fern allies using the anatomical and experimental approaches applied previously to woody taxa. In particular, we focused on the relationship between pit membrane traits and cavitation resistance at the level of the individual conduit.

## RESULTS

Large-diameter conduits, whether conifer tracheids or angiosperm vessels, are typically more vulnerable to cavitation than smaller ones (Hargrave et al., 1994; Cai and Tyree, 2010; Christman et al., 2011), so we looked for this trend across our assortment of ferns and fern allies (Table I) using a combination of anatomy and

conduit air injection to test for air-seeding thresholds (Choat et al., 2005). For the latter approach, a glass capillary was inserted into a conduit in a cut segment of the stipe (analogous to the petiole on a leaf), submerged in water, and progressively pressurized until air bubbled out the opposite end of the segment, indicating gas penetration through the largest pore in a pit membrane, that is the ASP (see "Materials and Methods"; Choat et al., 2006). The capillary method thus offers a proxy measurement for the negative pressure (i.e. hydrostatic tension) plants generate through transpiration and drought stress. ASPs were observed to vary from  $0.8 \pm 0.15$  MPa (mean  $\pm$  SD) in *Athyrium filix-femina*, a delicate, understory hydric species, to  $4.9 \pm 0.94$  MPa in *Psilotum nudum*, an early-derived epiphytic fern. The ASP averaged  $2.64 \pm 1.18$  MPa across the 12 species of seedless vascular plants sampled (Fig. 1). Interestingly, early-diverging taxa including *P. nudum*, *Selaginella pallescens*, and *Huperzia squarrosa* exhibited the highest ASPs, averaging  $4.3 \pm 0.53$  MPa. If we exclude the vessel-bearing *Pteridium aquilinum*, an increase in conduit diameter from 30 to 60  $\mu\text{m}$  was associated with a 5-fold drop in ASPs (Fig. 1;  $r^2 = 0.38$ ). In general, species with small-diameter tracheids were more resistant to membrane pore failure under increasing positive pressure in the conduit lumen.

Upon closer inspection, lower ASPs were associated with higher pit area per conduit wall (Fig. 2A;  $r^2 = 0.47$ ), with *P. aquilinum* emerging again as an outlier. Similar trends were observed between the area of a single pit aperture and ASP (Fig. 2B;  $r^2 = 0.41$ ). So altogether, these results imply that pit area is coupled to cavitation resistance in the xylem of seedless vascular plants in a manner that is functionally similar to angiosperms. Differences in species pit attributes could be readily visualized on macerated tracheids photographed under  $400\times$  (Fig. 3).

The rare-pit hypothesis of conduit air seeding is predicated on a probabilistic relationship between pit area and the presence of the large, rare pit membrane pore that facilitates air entry. It has been shown in several *Acer* species that, all else being equal, lower ASPs are required to push air through shorter stem segments than longer ones (Christman et al., 2009). This is because xylem in the longer stems is composed of a greater number

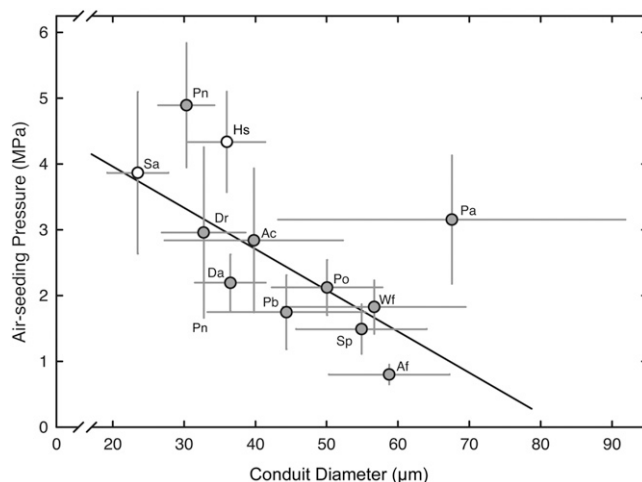


**Figure 1.** The relationship between mean conduit diameter and mean ASP in 10 species of ferns (gray circles) and two fern allies (white circles). Species with large-diameter tracheids were less resistant to increasing lumen air pressure. Error bars indicate SD;  $r^2 = 0.41$  excluding *P. aquilinum* (Pa). For species symbols, see Table 1.

of conduits per file and thus has a higher number of end walls that mask the effect of rare leaky pits (Choat and Pittermann, 2009; Christman et al., 2009). We observed no relationship between tracheid length and ASPs as well as no significant segment length effect in three ferns, where ASPs were equivalent across stipe segments ranging from 1 to 10 cm in length ( $P = 0.339$ ,  $0.388$ , and  $0.961$  for *Adiantum capillus-veneris*, *Polypodium aureum*, and *Woodwardia fimbriata*, respectively; Supplemental Figs. S1 and S2). This indicates that the distribution of large pores is very consistent between files of tracheids and that air seeding may be influenced by the presence of a large pore within the pit membrane of any one conduit.

Maximum pit membrane pore diameter ( $D$ ) was predicted from the ASPs with the Young-Laplace equation:

$$P = 4T \cos \alpha / D \quad (1)$$

where  $P$  is the ASP,  $T$  is the surface tension of water, and  $\alpha$  is the contact angle between the membrane microfibrils (assumed to be  $0^\circ$ ). Maximum pore diameter

**Table 1.** List of species used in this study and their collection sites, growth habits, and endemic habitats

Species	Family	Symbol	Collection Site	Habit	Endemic Habitat
<i>Adiantum capillus-veneris</i>	Pteridaceae	Ap	Glasshouse collection	Erect	North American warm-temperate forests
<i>Athyrium filix-femina</i>	Dryopteridaceae	Af	Coastal redwood forest	Erect	North American warm-temperate forests
<i>Dicksonia antarctica</i>	Dicksoniaceae	Da	Glasshouse collection	Erect	Southern hemisphere temperate forests
<i>Dryopteris arguta</i>	Dryopteridaceae	Dr	Coastal redwood forest	Erect	Western North American temperate forests
<i>Huperzia squarrosa</i>	Huperziaceae	Hs	Glasshouse collection	Erect	Tropical Australia
<i>Platycerium bifurcatum</i>	Polypodiaceae	Pb	Glasshouse collection	Epiphyte	Southeast Asia and subtropical Australia
<i>Polypodium aureum</i>	Polypodiaceae	Po	Glasshouse collection	Erect	North and South American tropical and subtropical forests
<i>Psilotum nudum</i>	Psilotaceae	Pn	Glasshouse collection	Erect	Hawaiian island tropical and subtropical regions
<i>Pteridium aquilinum</i>	Pteridaceae	Pa	Coastal redwood forest	Erect	Temperate and subtropical regions
<i>Selaginella pallescens</i>	Selaginellaceae	Sa	Glasshouse collection	Erect	North and South American tropical and subtropical forests
<i>Stenochlaena palustris</i>	Blechnaceae	Sp	Glasshouse collection	Epiphyte	India, China, Australia, and South Africa
<i>Woodwardia fimbriata</i>	Blechnaceae	Wf	Coastal redwood forest	Erect	Western North American temperate forests

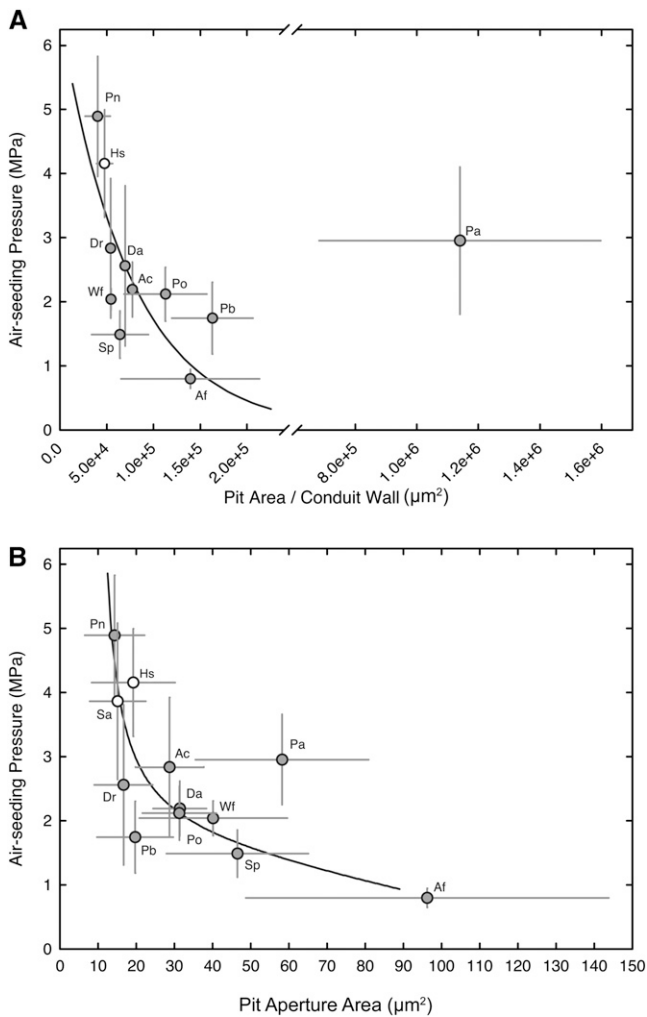


**Figure 2.** The relationship between mean conduit pit area (one wall; A), pit aperture area (B), and mean ASP for 10 fern species (gray circles) and two fern allies (white circles). Species with larger pit areas and pit aperture areas were less resistant to increasing lumen air pressure. Error bars indicate SD;  $r^2 = 0.74$  in A and  $0.47$  in B, both excluding *P. aquilinum* (Pa). For species symbols, see Table 1.

was found to correlate with the area of the pit aperture (Fig. 4;  $r^2 = 0.67$ ). Again, the two fern allies and *P. nudum* were tightly grouped at the low end of the range, and *A. filix-femina* had both the largest pit aperture area and the highest predicted pore size.

Given the close association between a species' pit membrane traits and ASPs, we endeavored to examine the pit membranes of select ferns and fern allies using transmission electron microscopy (Fig. 5). The micrographs reveal their pit membranes to vary with respect to density and thickness, but in general, we observed that membrane thickness ranges from  $0.22 \mu\text{m}$  in *A. filix-femina* to  $0.57 \mu\text{m}$  in *P. aquilinum*. Species with low ASPs such as *A. filix-femina*, *Stenochlaena palustris*, and *Platyce-rium bifurcatum* had the thinnest membranes, but beyond  $2 \text{ MPa}$ , the relationship between ASP and pit membrane

thickness was invariable (Fig. 6). Interestingly, *P. aquilinum* had the thickest pit membranes of all the sampled taxa, despite an intermediate ASP of  $2.96 \text{ MPa}$ . We suspect that this species' low ASP arises from its unusually high pit membrane area due to the presence of vessels (Fig. 2; see "Discussion").

Lastly, we estimated the area-based  $r_{\text{pit}}$  according to methods described by Wheeler et al. (2005) and Hacke et al. (2007), whereby lumen and pit membrane resistivities were partitioned from the total measured hydraulic resistivity on the basis of conduit anatomical traits, including lumen diameter, conduit length, and pit area (see "Materials and Methods"). Despite the variation in  $r_{\text{pit}}$  values, we observed a trend toward increasing  $r_{\text{pit}}$  with increasing ASP, with the  $r_{\text{pit}}$  of *A. filix-femina* being at the low end of the spectrum at  $3.88 \pm 3.25 \text{ MPa s m}^{-1}$ , while  $r_{\text{pit}}$  in *P. nudum* was estimated at  $81.03 \pm 32 \text{ MPa s m}^{-1}$ , consistent with an ASP of  $4.89 \text{ MPa}$  (Fig. 7A). Again, *P. aquilinum* was unusual, showing the highest estimated  $r_{\text{pit}}$  of  $282.9 \pm 129.5 \text{ MPa s m}^{-1}$ , a result possibly consistent with the thick pit membranes observed in this species (Fig. 6).

Taken together, the mean  $r_{\text{pit}}$  of our sampled seedless vascular plants was estimated at  $54.6 \text{ MPa s m}^{-1}$ , contributing on average 51% to transport resistance. This  $r_{\text{pit}}$  value drops slightly to  $49.5 \text{ MPa s m}^{-1}$  if data from Schulte et al. (1987) and Wheeler et al. (2005) are included. When compared across all tracheophytes, the pit membranes of seedless vascular plants have the second-highest  $r_{\text{pit}}$  after angiosperms, while the homogenous pit membranes of vesselless angiosperms and the torus-margo pits of conifers offer the lowest resistance to water flow (Fig. 7B). These results, along with those related to pit area and air seeding, imply that the structure and function of seedless vascular plant pit membranes resemble those of angiosperm pit membranes, despite the phylogenetic distance between these groups.

## DISCUSSION

Our data suggest that at the conduit level, cavitation resistance in seedless vascular plants is governed by the same principles as it is in the vessels of angiosperms. According to the rare-pit hypothesis, the probability of a developmental or stress-induced flaw resulting in a large, weak membrane pore increases with pit area and, thereby, conduit size (Wheeler et al., 2005; Hacke et al., 2006, 2007; Christman et al., 2009; Rockwell et al., 2014). Interestingly, ASPs across ferns and fern allies increase in smaller conduits, a trend that is related to smaller overall pit area as well as the area of a single pit aperture (Figs. 1 and 2). Hence, the rare-pit mechanism appears to operate in seedless vascular plants in a manner that is similar to that in angiosperms, probably because both groups employ homogenous pit membranes.

Among all the seedless vascular plants in this study, the geometry of the pits in the tracheid walls appeared to be more important in cavitation resistance than in any other measured trait. The strongest relationship we observed

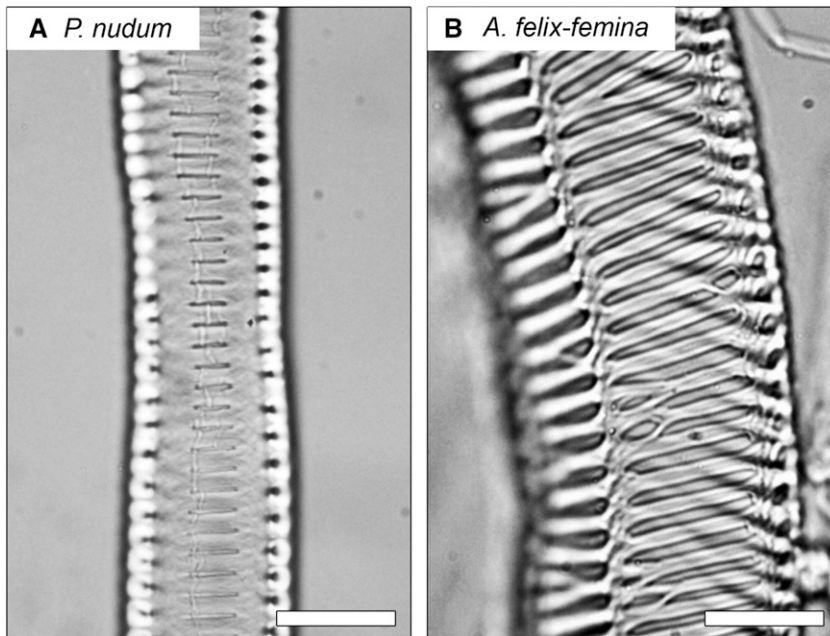


**Figure 3.** Longitudinal light micrographs of *P. nudum* (A) and *A. filix-femina* (B) conduits from macerations at 40 $\times$  magnification showing the differences in size and shape of the pit apertures. Species with smaller pit apertures (e.g. *P. nudum*) were more resistant to increasing lumen pressure than those with larger pit apertures. Bars = 10  $\mu$ m.

that helps explain the patterns in ASP across the 12 seedless vascular plants was pit aperture area ( $r^2 = 0.74$ ), suggesting that when more pit membrane area is exposed to the tracheid lumen, species become less resistant to air seeding. The most extreme example was *A. filix-femina*, which had large pit apertures and the highest ASP (Figs. 2A and 3B). In contrast, *P. nudum* had the smallest pit apertures and the lowest air-seeding threshold (Figs. 2A and 3A). While we did not consider other pit chamber characteristics in this study, previous work has shown that pit chamber depth appears to be related to air seeding in both conifers and some angiosperms and is likely related to the deflection distance and stretching of the pit membrane during an air-seeding event (Hacke and Jansen, 2009; Pittermann et al., 2010; Lens et al., 2011).

Despite the general trends between pit area and ASP, our data indicate that cavitation resistance can be acquired in a number of ways (Lens et al., 2011). Indeed, while pit area explained much of the variation in air seeding, the relationship between pit membrane thickness and ASP was less clear, despite the similarity in membrane thickness in both ferns and angiosperms (Fig. 6; Jansen et al., 2009; Lens et al., 2011). For example, only *A. filix-femina* and *S. palustris*, two species that are highly vulnerable to air seeding, showed conspicuously thinner pit membranes in comparison with the other taxa (Fig. 6). Beyond 2 MPa, however, membrane thickness was invariable across a range of ASPs, indicating that membrane area controls resistance to air seeding at higher pressures. Similar variation has been reported in angiosperm pit membranes, in which thickness and porosity are interrelated traits. While Hacke et al. (2006) and Wheeler et al. (2005) found no relationship between  $r_{\text{pit}}$  and cavitation resistance, the studies that examined membrane porosity directly with scanning and transmission electron microscopy suggest the opposite: thin, porous, and presumably low-resistance

membranes were more vulnerable to air seeding than thicker ones (Jansen et al., 2009; Lens et al., 2011). Xylem perfusion studies using solutions with variously sized particles both support (Jarbeau et al., 1995) and question (Choat et al., 2003) the relationship between membrane porosity and cavitation resistance, and the issue is even more obfuscated in primary xylem, in which abundant pit area may combine with porous membranes (Choat et al., 2005). Unless improvements in microscopy methods allow us to measure porosity directly, per Jansen et al. (2009), this trait may be intractable in the delicate, primary xylem of ferns and fern allies (Fig. 5; Carlquist and Schneider, 2001, 2007).

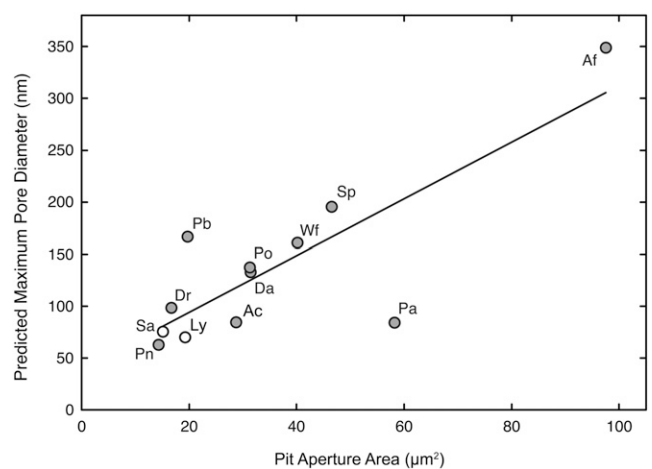


**Figure 4.** The relationship between pit aperture area and the predicted maximum pore diameter in pit membranes, as calculated from mean ASP values.  $r^2 = 0.67$ . For species symbols, see Table I.

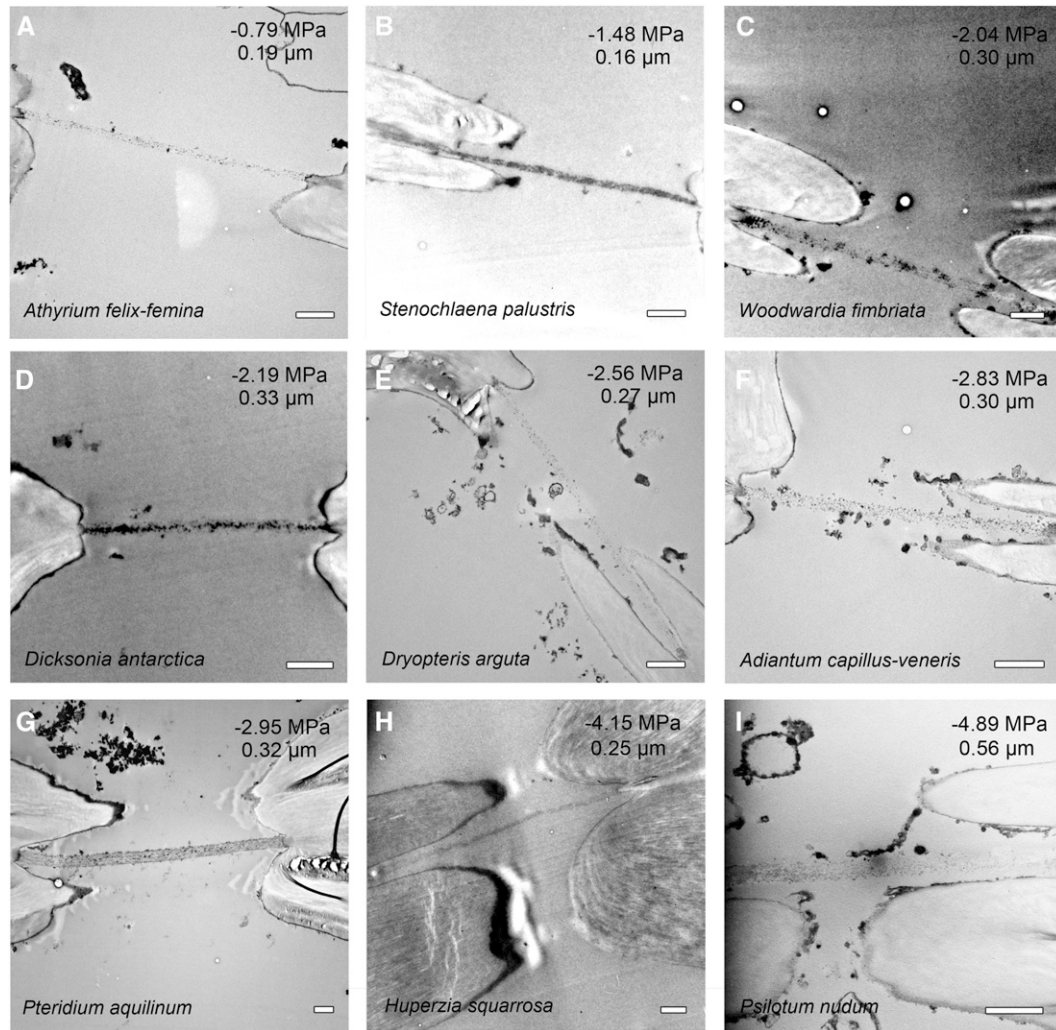


**Figure 5.** Representative transverse transmission electron micrographs showing pit membranes spanning the pit chamber in eight fern species and one lycophyte. A to I are arranged from highest (least pressure required) to lowest (most pressure required) mean ASP and their associated pit membrane thickness (given at top right). Bars = 1  $\mu\text{m}$ .

Although positive correlations have been reported between conduit size and hydraulic efficiency in terrestrial ferns, the classic tradeoff between hydraulic efficiency and cavitation safety was not observed when the cavitation response of the stipe was examined using either axial air injection or the centrifuge method (Watkins et al., 2010; Pittermann et al., 2011). However, our data show that this tradeoff convincingly exists at the level of the individual conduit (Fig. 1). What explains the absence of a tradeoff in previous studies? We suspect that variation in vascular bundle arrangements, in combination with pit membrane traits, may in part affect the spread of embolism within the stipe (Pittermann et al., 2011; Brodersen et al., 2012), as has been explored in angiosperms with the concept of the vessel grouping index and vascular sectoriality (Zanne et al., 2006; Schenk et al., 2008; Carlquist, 2009; Mencuccini et al., 2010; Lens et al., 2011; Martínez-Vilalta et al., 2012). For example, fronds of the fast-growing *P. aquilinum* have vascular bundles

that frequently bifurcate and fuse and are more vulnerable to embolism than species in which the bundles rarely come into contact, such as *W. fimbriata* (Brodersen et al., 2012). Presumably, the spread of embolism is more contained in a segregated vascular arrangement, but at the cost of hydraulic efficiency. One can easily imagine that, within a species, hierarchical variation in pit membrane traits, conduit size, conduit packing, connectivity, and bundle arrangement contribute to a complex cavitation response within the stipe (Brodersen et al., 2012; Pittermann et al., 2013). Since few species experience seasonal water potentials below  $-3$  MPa (Watkins et al., 2010; Brodersen et al., 2012; E.E. Burns, J. Pittermann, and C.J. Rico, unpublished data) and entire fronds appear to be quite vulnerable to cavitation (Brodrribb and Holbrook, 2004; McAdam and Brodrribb, 2013), the significance of the cavitation response in the stipe must also be carefully considered in the context of a species' life history strategy and microhabitat.

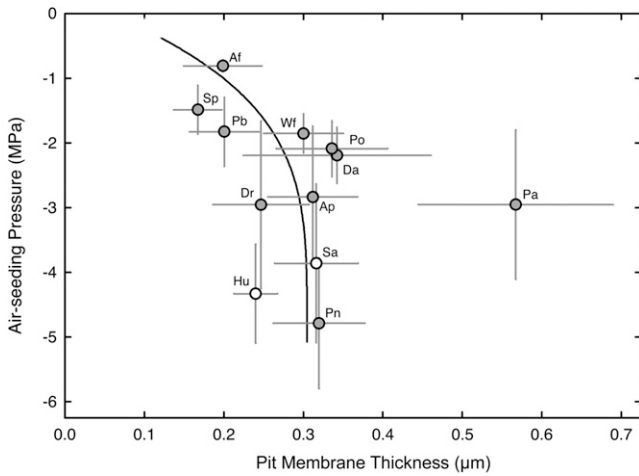


**Figure 6.** The relationship between mean pit membrane thickness and mean ASP in 10 fern species and two fern allies. Error bars indicate SD;  $r^2 = 0.40$  excluding *P. aquilinum* (Pa). For species symbols, see Table 1.

Surprisingly, conduit function in the vessel-bearing *P. aquilinum* differed from that in other ferns in every measurable way. Our anatomical data imply that *P. aquilinum* should have been one of the most vulnerable species to air seeding, given its large-diameter vessels, high pit area, and large pit apertures. Yet, *P. aquilinum* showed air-seeding thresholds that exceeded 3 MPa despite the presence of anatomical attributes that are expected to yield air-seeding thresholds of 1 MPa or lower. We suspect that *P. aquilinum*'s thick pit membranes are likely responsible for its high resistance to air seeding, as that trait stood out as one of the most striking features of this species compared with the other ferns. Membrane thickness may reflect greater microfibril density as well as a greater number of microfibril layers (Sperry and Hacke, 2004; Lee et al., 2012; Rockwell et al., 2014). Jansen et al. (2009) demonstrated a correlation between thicker pit membranes and smaller pore size in angiosperms, so selection may have favored thicker pit membranes in *P. aquilinum* in order to confer a much higher cavitation resistance than would otherwise be possible given the interconnectivity of its vascular bundles, its frequent vessels, and high pit area (Carlquist and Schneider, 2007; Pittermann et al., 2011, 2013; Brodersen et al., 2012).

In light of *P. aquilinum*'s vessels and distinctive pit membranes, it is interesting to consider the possibility that vessel evolution in ferns may have followed a parallel trajectory to vessel evolution in angiosperms, whereby the pit membranes in early-derived, tracheid-bearing angiosperm taxa show much higher porosity and lower  $r_{\text{pit}}$  than pit membranes belonging to vessels of more recently evolved eudicots (Hacke et al., 2007). In a case of convergent evolution, the development of thicker, less permeable, and more air seeding-resistant pit membranes in both angiosperms and *P. aquilinum* can be seen as an adaptation to reduce vulnerability to cavitation despite the higher pit area of vessels. Whether similar trends are

observed in other putatively vessel-bearing ferns (*Astrolepis*, *Marsilea*, and *Woodsia* spp.) remains to be seen (Carlquist and Schneider, 2007).

In the analysis of ASPs and area-based  $r_{\text{pit}}$ , we observed no clear relationship between these attributes in the sampled pteridophyte taxa, but as in previous studies on angiosperms and conifers (Pittermann et al., 2005, 2006; Wheeler et al., 2005; Hacke et al., 2007), our  $r_{\text{pit}}$  estimates are indirect, highly variable, and thus subject to error (Fig. 7A). Despite these caveats, our calculations encompass the range of published fern  $r_{\text{pit}}$  values on *P. nudum* and *P. aquilinum*, at 1.99 and 31 MPa s m<sup>-1</sup>, respectively (Schulte et al., 1987; Wheeler et al., 2005), and yield some valuable insights. For example, the  $r_{\text{pit}}$  of *P. aquilinum* is on par with values observed in many angiosperms and consistent with the thick membranes seen in this species (Figs. 5I and 6). Similarly, the higher

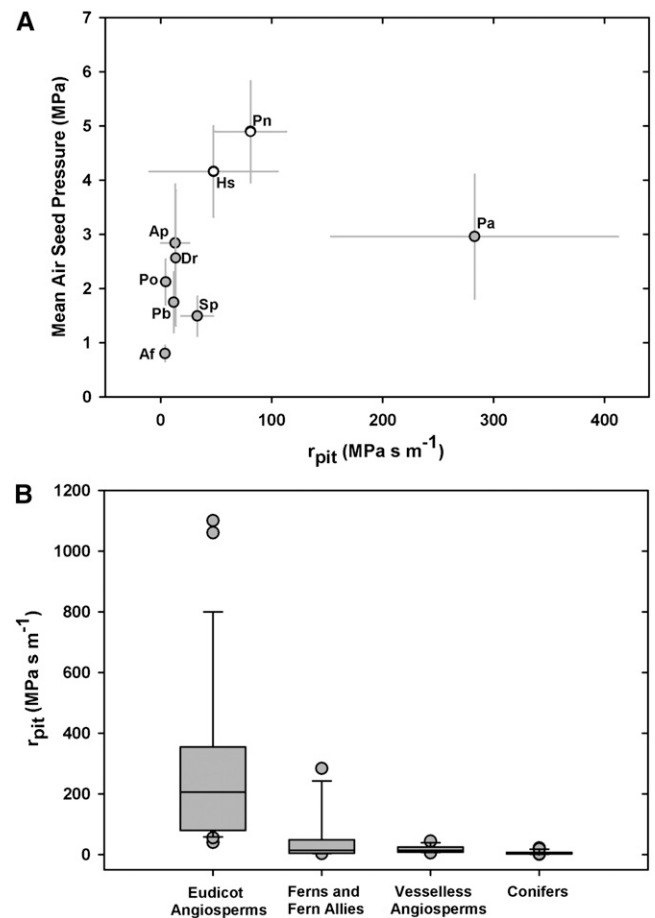


**Figure 7.** A, Area-based  $r_{\text{pit}}$  in ferns (gray circles) and fern allies (white circles) in relation to mean ASP. B, Box plots showing the  $r_{\text{pit}}$  of four functional plant types, where the box indicates the middle half of the sampled data, the line shows the sample median, and the whiskers show the upper and lower quarters of the distribution. Points outside the whisker range are considered outliers, such as *P. aquilinum* in the fern data set. Conifer data are from Pittermann et al. (2006), vesselless angiosperm data from Hacke et al. (2007), and vessel-bearing angiosperm data from Wheeler et al. (2005) and Hacke et al. (2006). Additional fern data are from Schulte et al. (1987) and Wheeler et al. (2005).

$r_{\text{pit}}$  values of *H. squarrosa* and *P. nudum* probably reflect their small pit apertures, evident in both light and transmission electron micrographs, and their generally high ASPs (Figs. 3 and 5, H and I). Certainly in the conifers, smaller pit apertures account for a large fraction of  $r_{\text{pit}}$  at increasingly lower water potentials and explain in part species' resistance to cavitation (Mayr et al., 2002; Burgess et al., 2006; Domec et al., 2008; Pittermann et al., 2010). Across all the seedless vascular taxa sampled in this study, end walls contributed  $51.25\% \pm 14.9\%$  (mean  $\pm$  SD) to transport resistance, with lumen resistance accounting for the balance. When data from Schulte et al. (1987; 43%) and Wheeler et al. (2005; 50%) are included, this average is essentially unchanged at 51%, which is quite similar to the average 56% wall resistivity computed for angiosperms (Wheeler et al., 2005; see also Gibson et al., 1985). Lastly, when examined across all functional plant groups, the homogenous pit membranes of angiosperms exhibit the highest range of  $r_{\text{pit}}$  values, with the pit membranes of seedless vascular plants ranking second, at a mean  $r_{\text{pit}}$  of  $49.5 \text{ MPa s m}^{-1}$  (including data from Wheeler et al. [2005] and Schulte et al. [1987]), and dropping to  $11.81 \text{ MPa s m}^{-1}$  if early-diverging seedless vascular plants (*P. nudum* and *H. squarrosa*) and *P. aquilinum* are excluded (Fig. 7B). Our data suggest that, much as in vesselless angiosperms and conifers, permeable pit membranes in basal tracheophytes compensate in part for the higher resistance imposed by a tracheid-based vascular system (Pittermann et al., 2005; Hacke et al., 2007).

## CONCLUSION

Despite their ancient origins, it appears that early-derived vascular plants have xylem that is adaptive with respect to both hydraulic function and cavitation resistance (Watkins et al., 2010; Pittermann et al., 2011, 2013). Indeed, pit area is an identified trait that influences air seeding in both seedless vascular plants and angiosperms, suggesting that selection acted on homogenous pit membranes in a largely convergent manner. In the primary xylem of seedless vascular plants, where many pits span the length of the tracheid, it is not surprising that membrane thickness also varies, as shown in the more vulnerable taxa and the vessel-bearing outlier, *P. aquilinum* (Fig. 6). Further sampling of terrestrial and epiphytic taxa, as well as other members of the Lycopodiopsida, from their native habitats may provide a more nuanced perspective, since, contrary to what we observed, one might expect frequent epiphytes, such as *P. nudum*, *S. palustris*, and *P. bifurcatum*, to exhibit greater air-seeding resistance than taxa growing in soil (Watkins et al., 2010). Species' phylogenetic position may also contribute to the story, since basal taxa such as *S. pallescens*, *H. squarrosa*, and *P. nudum* have the most air seeding-resistant conduits among the seedless vascular plants we sampled. Certainly, these species have the least room for error during water deficit, since their small amount of xylem is contained in a single, central bundle (protostele)

with none of the vascular redundancy found in more derived taxa (Pittermann et al., 2011, 2013; Brodersen et al., 2012). Lastly, pit area resistance in seedless vascular plants is variable but on par with the range of values published in previous studies and in vesselless angiosperms (Schulte et al., 1987; Wheeler et al., 2005; Hacke et al., 2007). Low wall resistance combined with large-diameter, tightly packed tracheids serves to improve hydraulic efficiency in seedless vascular plants, despite their meager amounts of primary xylem (Pittermann et al., 2013), while the considerable air-seeding resistance of their conduits may protect the xylem from hydraulic failure (Watkins et al., 2010; Pittermann et al., 2011; Brodersen et al., 2012). Despite the narrow range of water potentials under which most ferns operate (McAdam and Brodrribb, 2013), we suspect that numerous, though perhaps subtle, permutations of physiological and life history traits have contributed to the diversity of seedless vascular plants and may help explain their persistence over time and space.

## MATERIALS AND METHODS

### Plant Material and Collection

For this study, we chose 10 fern species and two species of lycophytes representing a broad range in morphology, phylogeny, ontogeny, and habitat preference (Table I).

### Transmission Electron Microscopy

Fresh material was collected from the University of California Santa Cruz campus or greenhouse collection, wrapped in wet tissue, put in zip-seal bags, and express shipped to Ulm University. Small segments of  $1 \text{ mm}^3$  of vascular tissue were prepared using a stereomicroscope. After washing in 0.2 M phosphate buffer at pH 7.3, the specimens were postfixed in 2% (w/v) buffered osmium tetroxide for 1 to 2 h at room temperature, washed again, and dehydrated through a graded ethanol series (30%, 50%, and 70%), followed by 90% propanol. Afterward, the specimens were stained with 118 mM uranyl acetate dissolved in ethanol for at least 30 min at 37°C and then rinsed three times with 100% propanol. The propanol was replaced by propylene oxide, which was gradually replaced with Epon resin (Sigma-Aldrich) using a 2:1 solution for 15 min, 30 min at 1:1, 1 h at 1:2, and overnight in 100% Epon at room temperature. The Epon resin was then replaced once again and polymerized at 60°C for 48 h. Embedded samples were trimmed with a razor blade and sectioned with an ultramicrotome (UltraCut; Reichert-Jung). Transverse sections of 1 to 2  $\mu\text{m}$  thick were cut with a glass knife, heat fixed to glass slides, stained with 0.5% (w/v) Toluidine Blue O in 0.1 M phosphate buffer, and mounted in DPX, which is a mixture of distyrene, dibutylphthalate and xylene (Agar Scientific). Resin-embedded material was prepared for transmission electron microscopy by cutting transverse, ultrathin sections between 60 and 90 nm using a diamond knife. The sections were attached to 300-mesh hexagonal copper grids (Agar Scientific) and stained manually with lead citrate for 1 min. Observations were carried out on transverse sections using a JEOL 1400 transmission electron micrograph at 80 kV accelerating voltage.

### Conduit Macerations

Stipe or stem segments were cut from field- or greenhouse-grown plants collected from the University of California Santa Cruz campus and returned to the laboratory. Plant tissue surrounding the vascular bundles was carefully removed, and the bundles were placed into glass vials with a 1:1 mixture of 80% glacial acetic acid and 30% hydrogen peroxide per Mauseth and Fujii (1994) and maintained at 90°C for up to 7 d. Once the vascular bundles had cleared, they were rinsed in deionized water, and the tracheids were separated, mounted on glass slides, and photographed under 20 $\times$  to 40 $\times$  using a compound microscope and digital camera (BA 400; Motic). Conduit length, pit aperture, pit height, pit width, and functional xylem area were measured using ImageJ software (<http://imagej.nih.gov/ij/>).

## ASP

To determine the pressure required to push air across pit membranes between adjacent individual conduits (ASP), we followed the methods of Choat et al. (2005), where the positive pressure applied to the conduit is equal to but the opposite sign of the tension necessary to pull air from a neighboring air-filled conduit into a functional one. Stipe segments were collected from field- or greenhouse-grown plants on the University of California Santa Cruz campus. Segments were trimmed underwater to 6 cm for most species, but it was necessary to use longer segments (up to 15 cm) for *P. aquilinum* and *D. arguta* in order to locate conduits that did not span the entire length of the segment without an end wall or that were unusually vulnerable to air seeding. Segments were then secured in a multipoint articulating vise (no. 209; Panavise), and the cut transverse surface was viewed with a dissecting microscope. A digital photograph was then taken of the transverse surface, and a conduit was selected for capillary tube insertion. Next, a glass microcapillary tube pulled to a tip diameter of approximately 15  $\mu\text{m}$  was inserted by hand into a single conduit. The microcapillary tube was then sealed in place using a cyanoacrylic glue (Loctite no. 409; Henkel) and hardening accelerant (Loctite no. 7452). The microcapillary tube was then mounted in a modified capillary tube holder (Stoelting) attached to a 1-m length of PEEK tubing with its terminus located in a Scholander-style pressure chamber (PMS Instruments). The capillary holder was mounted on a ring stand such that the distal end of the segment was below the surface of the water in a 500-mL Pyrex beaker. Low pressure was then applied to the conduit (less than 0.05 MPa). If air bubbles were visibly exiting the distal end of the stem, it was determined that the conduit spanned the entire length of the segment and the segment was discarded. Next, the pressure was increased at a rate of 0.5 MPa  $\text{min}^{-1}$  until air bubbles were observed exiting the distal end of the segment. The positive pressure at this point was recorded as the ASP. Air-seeding measurements were made for 10 different segments for each species. Following successful ASP measurement, the digital image of the transverse face was used to measure the diameter of the conduit. In this way, we were able to analyze the relationship between ASP and conduit diameter.

To determine whether the air-seeding measurements were influenced by sample length, we selected three species (*A. capillus-veneris*, *P. aureum*, and *W. fimbriata*) for independent study. For each species, stipes were cut to create five segments for each of the following length categories: 1, 2, 4, 6, and 10 cm. The air-seeding threshold was then determined for each of those segments.

## Calculation of Area-Specific $r_{\text{pit}}$

We estimated  $r_{\text{pit}}$  according to the methods of Wheeler et al. (2005), who based their approach in part on Schulte and Gibson (1988). Usefully, Wheeler et al. (2005) computed  $r_{\text{pit}}$  for *P. aquilinum*, while Schulte et al. (1987) achieved this for *P. nudum*.

To first determine xylem-specific conductivity ( $K_C$ ), six fronds from each species were cut from the field or greenhouse, recut underwater in the laboratory, and then degassed overnight under house vacuum in 20 mM KCl solution to remove any native embolism. Stipe segments were then cut to 14.5 cm in length for *A. capillus-veneris*, *A. filix-femina*, *D. antarctica*, *D. arguta*, *P. aureum*, *P. aquilinum*, *P. bifurcatum*, and *W. fimbriata*. Segments of *H. squarrosa*, *P. nudum*, and *S. palustris* were cut to a length of 6 cm to exclude any nodes in the segments. Maximum hydraulic conductivity ( $K_{\text{max}}$ ) was measured following the methods of Hacke et al. (2000) and calculated as a function of the flow rate through the section at a given pressure. Segments were mounted in a tubing apparatus to direct the flow of a 20 mM KCl solution through the xylem at a pressure of 6 to 8 kPa to measure  $K_{\text{max}}$  after degassing. The flow rate through the sections without a pressure head was measured before and after each gravimetric measurement to control for equilibrium drift in the system. These background measurements were averaged and subtracted from the pressure-induced flow rates. Thin, handmade cross sections of the stipes were photographed, and the xylem area was measured using ImageJ software.  $K_{\text{max}}$  was then divided by the xylem area to yield  $K_C$ .

The calculation of  $r_{\text{pit}}$  first assumes that conduit resistivity ( $R_C$ ;  $\text{m}^{-4}$  MPa s;  $R_C = 1/K_C$ ) is the sum of the mean lumen resistivity ( $R_L$ ;  $\text{m}^{-4}$  MPa s) and the mean end wall resistivity ( $R_{W_e}$ ;  $\text{m}^{-4}$  MPa s), such that:

$$R_C = R_L + R_{W_e} \quad (2)$$

$R_L$  was estimated from conduit diameter measurements from all the conduits observed within a cross section of the frond stipe. All anatomical data were collected on fronds on which  $R_C$  was determined. Transverse hand sections were stained with phloroglucinol (Sigma-Aldrich), mounted on a glass slide with glycerin, and photographed. We computed the equivalent circle diameter

for all measured conduits because conduit shapes were irregular. The Hagen-Poiseuille conductivities of each conduit were summed to obtain the total lumen area-specific conductivity, the inverse of which was then expressed as the xylem area-specific  $R_L$ .  $R_L$  was then multiplied by the conduit density (no. of conduits/ $\text{m}^2$ ) to obtain the  $R_L$  of the average conduit. Ultimately, the average  $R_{W_e}$  was computed as  $R_C$  minus  $R_L$ .

In angiosperms, the end wall resistance ( $r_w$ ;  $\text{m}^{-3}$  MPa s) is calculated by multiplying  $R_{W_e}$  by  $L'$  (m), which is the length between conduit end walls (Wheeler et al., 2005). Across all species,  $L'$  was determined by multiplying the average conduit length,  $L$ , by 0.5 per Wheeler et al. (2005).  $L$  was determined on entire conduits separated according to the maceration procedure of Mauseth and Fujii (1994) as described above. Pittermann et al. (2011) estimated mean conduit length in *P. aquilinum* using silicon injections, so we used their data since the fronds were of similar size and collected at the same location. Conduits were photographed in their entirety, and the  $L$  was measured using ImageJ software.

Area-specific  $r_{\text{pit}}$  ( $\text{MPa s m}^{-1}$ ) was then estimated as:

$$r_{\text{pit}} = r_w \times A_p / 2 \quad (3)$$

where  $A_p$  ( $\text{m}^2$ ) is the average pit membrane area.  $A_p$  was estimated by directly measuring the pit membrane area of the conduits on which  $L$  was determined. Conduit-to-conduit contact is highly variable in ferns, so we assumed that two conduit walls were pitted, as in the vessels and tracheids of woody plants (Wheeler et al., 2005; Hacke et al., 2006).

## Supplemental Data

The following materials are available in the online version of this article.

**Supplemental Figure S1.** Mean ASP values for three fern species.

**Supplemental Figure S2.** Mean ASP and tracheid diameter compared with mean tracheid length.

## ACKNOWLEDGMENTS

We thank the Electron Microscopy section of Ulm University for assistance with preparing transmission electron microscopy samples and the anonymous reviewers whose helpful comments and suggestions improved the article.

Received August 10, 2013; accepted April 13, 2014; published April 28, 2014.

## LITERATURE CITED

- Brodersen CR, McElrone AJ, Choat B, Lee EF, Shackel KA, Matthews MA** (2013) In vivo visualizations of drought-induced embolism spread in *Vitis vinifera*. *Plant Physiol* **161**: 1820–1829
- Brodersen CR, Roark LC, Pittermann J** (2012) The physiological implications of primary xylem organization in two ferns. *Plant Cell Environ* **35**: 1898–1911
- Brodribb TJ, Holbrook NM** (2004) Stomatal protection against hydraulic failure: a comparison of co-existing ferns and angiosperms. *New Phytol* **162**: 663–670
- Burgess SSO, Pittermann J, Dawson TE** (2006) Hydraulic efficiency and safety of branch xylem increases with height in *Sequoia sempervirens* (D. Don) crowns. *Plant Cell Environ* **29**: 229–239
- Cai J, Tyree MT** (2010) The impact of vessel size on vulnerability curves: data and models for within-species variability in saplings of aspen, *Populus tremuloides* Michx. *Plant Cell Environ* **33**: 1059–1069
- Carlquist S** (2009) Non-random vessel distribution in woods: patterns, modes, diversity correlations. *Aliso* **27**: 39–58
- Carlquist S, Schneider EL** (2001) Vessels in ferns: structural, ecological, and evolutionary significance. *Am J Bot* **88**: 1–13
- Carlquist S, Schneider EL** (2007) Tracheary elements in ferns: new techniques, observations and concepts. *Am Fern J* **97**: 199–211
- Choat B, Ball M, Lully J, Holtum J** (2003) Pit membrane porosity and water stress-induced cavitation in four co-existing dry rainforest tree species. *Plant Physiol* **131**: 41–48
- Choat B, Brodie TW, Cobb AR, Zwieniecki MA, Holbrook NM** (2006) Direct measurements of intervessel pit membrane hydraulic resistance in two angiosperm tree species. *Am J Bot* **93**: 993–1000

- Choat B, Cobb AR, Jansen S (2008) Structure and function of bordered pits: new discoveries and impacts on whole-plant hydraulic function. *New Phytol* **177**: 608–625
- Choat B, Jansen S, Brodrribb TJ, Cochard H, Delzon S, Bhaskar R, Bucci SJ, Feild TS, Gleason SM, Hacke UG, et al (2012) Global convergence in the vulnerability of forests to drought. *Nature* **491**: 752–755
- Choat B, Lahr EC, Melcher PJ, Zwieniecki MA, Holbrook NM (2005) The spatial pattern of air seeding thresholds in mature sugar maple trees. *Plant Cell Environ* **28**: 1082–1089
- Choat B, Pittermann J (2009) New insights into bordered pit structure and cavitation resistance in angiosperms and conifers. *New Phytol* **182**: 557–560
- Christman MA, Sperry JS, Adler FR (2009) Testing the 'rare pit' hypothesis for xylem cavitation resistance in three species of *Acer*. *New Phytol* **182**: 664–674
- Christman MA, Sperry JS, Smith DD (2011) Rare pits, large vessels and extreme vulnerability to cavitation in a ring-porous species. *New Phytol* **193**: 713–720
- Delzon S, Douthe C, Sala A, Cochard H (2010) Mechanism of water-stress induced cavitation in conifers: bordered pit structure and function support the hypothesis of seal capillary-seeding. *Plant Cell Environ* **33**: 2101–2111
- Domec JC, Lachenbruch B, Meinzer FC (2006) Bordered pit structure and function determine spatial patterns of air-seeding thresholds in xylem of Douglas-fir (*Pseudotsuga menziesii*; Pinaceae) trees. *Am J Bot* **93**: 1588–1600
- Domec JC, Lachenbruch B, Meinzer FC, Woodruff DR, Warren JM, McCulloh KA (2008) Maximum height in a conifer is associated with conflicting requirements for xylem design. *Proc Natl Acad Sci USA* **105**: 12069–12074
- Gibson AC, Calkin HW, Nobel PS (1985) Hydraulic conductance and xylem structure in tracheid-bearing plants. *IAWA J* **6**: 293–302
- Hacke UG, Jansen S (2009) Embolism resistance of three boreal conifer species varies with pit structure. *New Phytol* **182**: 675–686
- Hacke UG, Sperry JS, Feild TS, Sano Y, Sikkema EH, Pittermann J (2007) Water transport in vesselless angiosperms: conducting efficiency and cavitation safety. *Int J Plant Sci* **168**: 1113–1126
- Hacke UG, Sperry JS, Pittermann J (2000) Drought experience and cavitation resistance in six shrubs from the Great Basin, Utah. *Basic Appl Ecol* **1**: 31–41
- Hacke UG, Sperry JS, Wheeler JK, Castro L (2006) Scaling of angiosperm xylem structure with safety and efficiency. *Tree Physiol* **26**: 689–701
- Hargrave KR, Kolb KJ, Ewers FW, Davis SD (1994) Conduit diameter and drought-induced embolism in *Salvia mellifera* Greene (Labiatae). *New Phytol* **126**: 695–705
- Hubbard RM, Stiller V, Ryan MG, Sperry JS (2001) Stomatal conductance and photosynthesis vary linearly with plant hydraulic conductance in ponderosa pine. *Plant Cell Environ* **24**: 113–121
- Jansen S, Choat B, Pletsers A (2009) Morphological variation of intervessel pit membranes and implications to xylem function in angiosperms. *Am J Bot* **96**: 409–419
- Jansen S, Lamy JB, Burlett R, Cochard H, Gasson P, Delzon S (2012) Plasmodesmatal pores in the torus of bordered pit membranes affect cavitation resistance of conifer xylem. *Plant Cell Environ* **35**: 1109–1120
- Jarbeau JA, Ewers FW, Davis SD (1995) The mechanism of water-stress-induced embolism in two species of chaparral shrubs. *Plant Cell Environ* **18**: 189–196
- Lee J, Holbrook NM, Zwieniecki MA (2012) Ion induced changes in the structure of bordered pit membranes. *Front Plant Sci* **3**: 55
- Lens F, Sperry JS, Christman MA, Choat B, Rabaey D, Jansen S (2011) Testing hypotheses that link wood anatomy to cavitation resistance and hydraulic conductivity in the genus *Acer*. *New Phytol* **190**: 709–723
- Martínez-Vilalta J, Mencuccini M, Alvarez X, Camacho J, Loepele L, Piñol J (2012) Spatial distribution and packing of xylem conduits. *Am J Bot* **99**: 1189–1196
- Mauseth JD, Fujii T (1994) Resin-casting: a method for investigating apoplastic spaces. *Am J Bot* **81**: 104–110
- Mayr S, Wolfschwenger M, Bauer H (2002) Winter-drought induced embolism in Norway spruce (*Picea abies*) at the alpine timberline. *Physiol Plant* **115**: 74–80
- McAdam SAM, Brodrribb TJ (2013) Ancestral stomatal control results in a canalization of fern and lycophyte adaptation to drought. *New Phytol* **198**: 429–441
- Mencuccini M, Martínez-Vilalta J, Piñol J, Loepele L, Burnat M, Alvarez X, Camacho J, Gil D (2010) A quantitative and statistically robust method for the determination of xylem conduit spatial distribution. *Am J Bot* **97**: 1247–1259
- Morrow AC, Dute RR (1998) Development and structure of pit membranes in the rhizome of the woody fern *Botrychium dissectum*. *IAWA J* **19**: 429–441
- Pesacreta TC, Groom LH, Rials TG (2005) Atomic force microscopy of the intervessel pit membrane in the stem of *Sapium sebiferum* (Euphorbiaceae). *IAWA J* **26**: 397–426
- Pittermann J, Brodersen C, Watkins JE (2013) The physiological resilience of fern sporophytes and gametophytes: advances in water relations offer new insights into an old lineage. *Front Plant Sci* **5**: 285
- Pittermann J, Choat B, Jansen S, Stuart SA, Lynn L, Dawson TE (2010) The relationships between xylem safety and hydraulic efficiency in the Cupressaceae: the evolution of pit membrane form and function. *Plant Physiol* **153**: 1919–1931
- Pittermann J, Limm E, Rico C, Christman MA (2011) Structure-function constraints of tracheid-based xylem: a comparison of conifers and ferns. *New Phytol* **192**: 449–461
- Pittermann J, Sperry JS, Hacke UG, Wheeler JK, Sikkema EH (2005) Torus-margo pits help conifers compete with angiosperms. *Science* **310**: 1924
- Pittermann J, Sperry JS, Hacke UG, Wheeler JK, Sikkema EH (2006) Inter-tracheid pitting and the hydraulic efficiency of conifer wood: the role of tracheid allometry and cavitation protection. *Am J Bot* **93**: 1265–1273
- Plavcová L, Jansen S, Klepsch M, Hacke UG (2013) Nobody's perfect: can irregularities in pit structure influence vulnerability to cavitation. *Front Plant Sci* **4**: 453
- Rockwell FE, Wheeler JK, Holbrook NM (2014) Cavitation and its discontents: opportunities for resolving current controversies. *Plant Physiol* **164**: 1649–1660
- Schenk JH, Espino S, Goedhart CM, Nordenstahl M, Martínez Cabrera HI, Jones CS (2006) Hydraulic integration and shrub growth form linked across continental aridity gradients. *Proc Natl Acad Sci USA* **105**: 11248–11253
- Scholz A, Rabaey D, Stein A, Cochard H, Smets E, Jansen S (2013) The evolution and function of vessel and pit characters with respect to cavitation resistance across 10 *Prunus* species. *Tree Physiol* **33**: 684–694
- Schulte PJ (2012) Computational fluid dynamics models of conifer bordered pits show how pit structure affects flow. *New Phytol* **193**: 721–729
- Schulte PJ, Gibson AC (1988) Hydraulic conductance and tracheid anatomy in six species of extant seed plants. *Can J Bot* **66**: 1073–1079
- Schulte PJ, Gibson AC, Nobel P (1987) Xylem anatomy and hydraulic conductance of *Psilotum nudum*. *Am J Bot* **74**: 1438–1445
- Schymanski SJ, Or D, Zwieniecki M (2013) Stomatal control and leaf thermal and hydraulic capacitances under rapid environmental fluctuations. *PLoS ONE* **8**: e54231
- Sperry JS, Hacke UG (2004) Analysis of circular bordered pit function: I. Angiosperm vessels with homogenous pit membranes. *Am J Bot* **91**: 369–385
- Sperry JS, Hacke UG, Pittermann J (2006) Size and function in conifer tracheids and angiosperm vessels. *Am J Bot* **93**: 1490–1500
- Tyree MT, Sperry JS (1988) Do woody plants operate near the point of catastrophic dysfunction caused by dynamic water stress? Answers from a model. **88**: 574–580
- Watkins JE Jr, Holbrook NM, Zwieniecki MA (2010) Hydraulic properties of fern sporophytes: consequences for ecological and evolutionary diversification. *Am J Bot* **97**: 2007–2019
- Wheeler JW, Sperry JS, Hacke UG, Hoang N (2005) Intervessel pitting and cavitation in woody Rosaceae and other vesseled plants: a basis for a safety vs. efficiency trade-off in xylem transport. *Plant Cell Environ* **28**: 800–812
- Zanne AE, Sweeney K, Sharma M, Orians CM (2006) Patterns and consequences of differential vascular sectoriality in 18 temperate tree and shrub species. *Funct Ecol* **20**: 200–206
- Zimmermann M, Tyree MT (2002) *Xylem Structure and the Ascent of Sap*. Springer-Verlag, Berlin